



Co-existence of airborne SARS-CoV-2 infection and non-infection in three connected zones of a restaurant

Wei Jia^a, Qun Wang^b, David Christopher Lung^{c, d}, Pak-To Chan^a, Peihua Wang^e,
Edwin Chung-Hin Dung^a, Tiffany Didik^{c, d}, Garnet Kwan-Yue Choi^d, Herman Tse^d, Yijie Wu^f,
Te Miao^a, Wenzhao Chen^a, Hua Qian^g, Fan Xue^f, Yuguo Li^{a, h, *}

^a Department of Mechanical Engineering, The University of Hong Kong, Hong Kong, China

^b National Observation and Research Station of Coastal Ecological Environments in Macao, Macao Environmental Research Institute, Macau University of Science and Technology, Taipa, Macao 999078, China

^c Department of Pathology, Queen Elizabeth Hospital, Hong Kong, China

^d Department of Pathology, Hong Kong Children's Hospital, Hong Kong, China

^e Department of Epidemiology, Mailman School of Public Health, Columbia University, New York, USA

^f Department of Real Estate and Construction, The University of Hong Kong, Hong Kong, China

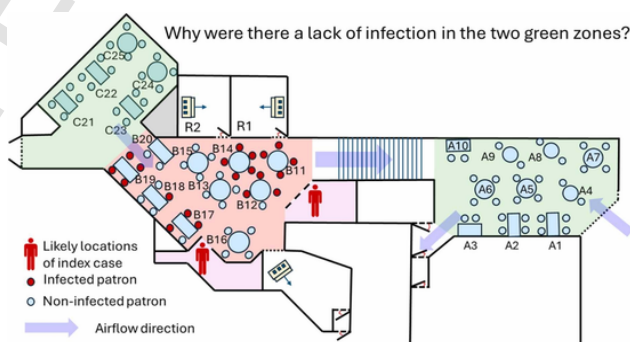
^g School of Energy and Environment, Southeast University, Nanjing, China

^h Faculty of Architecture, The University of Hong Kong, Hong Kong, China

HIGHLIGHTS

- A SARS-CoV-2 outbreak was reported with confined infections.
- Whole-genome sequencing revealed that a single source outbreak.
- The largest-to-date quanta generation rate of 1968 quanta/h was determined.
- Lack of infection in the other two zones was explained.
- Infection prevention was not achieved by ventilation alone.

GRAPHICAL ABSTRACT



ARTICLE INFO

Keywords:

Airborne transmission
Minimum ventilation requirement
FCU filtration
COVID-19
Quanta generation rate

ABSTRACT

The lack of knowledge on quanta generation rates presents a major obstacle to specifying the minimum ventilation required to prevent airborne infections. The expected largest quanta generation rate of severe acute respiratory syndrome coronavirus 2 (SARS-CoV-2) by a super-spreader remains unknown. Here we investigated a SARS-CoV-2 outbreak during lunch in a restaurant using epidemiological, whole-genome sequencing and environmental analyses. Both tracer gas and fine particles were used in field experiments to quantify aerosol dispersion and removal across three interconnected zones: Zone A, Zone B and Zone C. All 21 secondary patron infections occurred in Zone B. This unique infection feature and measured dilution flow rates allowed us to estimate the largest reported quanta generation rates to date, ranging from 1724 to 1968 quanta/h. These rates were sufficiently high to cause a high attack rate in Zone B but did not cause infections in Zones A and C, likely due to suffi-

* Corresponding author at: Department of Mechanical Engineering, The University of Hong Kong, Hong Kong, China
E-mail address: liy@hku.hk (Y. Li).

<https://doi.org/10.1016/j.jhazmat.2024.136388>

Received 29 August 2024; Received in revised form 14 October 2024; Accepted 31 October 2024

0304-3894/© 20XX

This is the peer-reviewed post-print version of the paper:

Jia, W., Wang, Q., Lung, D. C., Chan, P. T., Wang, P., Dung, E. C.-H., Didik, T., Choi, G. K.-Y., Tse, H., Wu, Y., Miao, T., Chen, W., Qian, H., Xue, F., & Li, Y. (2024). Co-existence of airborne SARS-COV-2 infection and non-infection in three connected zones of a restaurant. *Journal of Hazardous Materials*, 480: 136388. <https://doi.org/10.1016/j.jhazmat.2024.136388>.

The final version of this paper is available at: <https://doi.org/10.1016/j.jhazmat.2024.136388>. The use of this file must follow the Creative Commons Attribution Non-Commercial No Derivatives License, as required by Elsevier's policy.

cient dilution and insignificant contaminated airflow from Zone B, respectively. Our finding of the largest quanta generation rate so far suggests that avoiding secondary infection by dilution alone in the presence of a super-emitter might not be possible in typical air-conditioned buildings and other prevention strategies need to be developed.

1. Introduction

The airborne transmission of viruses such as influenza and severe acute respiratory syndrome coronavirus 2 (SARS-CoV-2) in crowded and poorly ventilated indoor environments has increasingly drawn attention [26,30,43]. The importance of a sufficient ventilation rate has been demonstrated in several studies (e.g., [33,38]). In terms of infection control efficacy and economic efficiency for pandemic intervention, it is necessary to specify the minimum required equivalent ventilation rate for avoiding airborne transmission. However, this rate remains unknown due to uncertainty about quanta generation rates, which refer to the hourly number of infectious quanta produced by the infected source persons (i.e. index cases). A quantum is defined as the number of virus particles needed to produce a probability of 63.2 % of infecting a susceptible individual [44]. For many years, quanta generation rates have been estimated using outbreak data based on the Wells–Riley equation [34]. Typically, values between 30 and 1000 quanta/h have been estimated for SARS-CoV-2 [29,31]. In most studies of potentially airborne outbreaks of respiratory infection, there has been a lack of ventilation rate measurement, possibly due to difficulties in full access to the involved venues and the lack of a simple but effective measurement method. Among infected individuals, the ability to expire infectious viruses is variable and thus heterogeneous. By integrating the viral load method of Buonanno et al. [4] with outbreak data, Cheng et al. [48] recently reported a population profile of quanta generation rates for ancestral SARS-CoV-2, with an expected quanta generation rate of at least 2300 quanta/h for the top 1% of infected individuals. Such a high quanta generation rate has not been identified in previously reported outbreaks, although very high attack rates have been reported in many studies [2,8,22]. A lack of ventilation data has prohibited the estimation of quanta generation associated with those outbreaks.

Given the importance of ventilation data in estimating quanta generation rates, this study investigates a specific SARS-CoV-2 outbreak to see how equivalent ventilation rate and airflow patterns affect virus transmission in a real-world setting. In this paper, we report a detailed epidemiological and environmental study of a restaurant outbreak of SARS-CoV-2 infection in Hong Kong. In this event, 21 of 76 patrons, four of eight kitchen staff and six of 11 waiters became infected with SARS-CoV-2 from the index case, an older male cleaner. The involved restaurant has two major dining areas: the first floor (Zone A), which has a main entrance to a shopping centre, and a lower (ground) floor; the dining areas are connected by a staircase. The lower floor can be further divided into two zones: Zones B and C. All 21 secondarily infected patrons had lunch in Zone B between 1 and 3 p.m. on 19 February 2021, while no patrons dining in Zones A and C at the same time became infected. During 5–10 March 2021, we performed detailed measures of field airflow in the restaurant, including the air change rates, dispersion of tracer gas and fine particles and bidirectional flow between the first and lower floors, with the original layout of tables. Shortly after this outbreak, mandatory dilution legislature was enacted in Hong Kong to reduce the risk of indoor SARS-CoV-2 transmission. A minimum of six air changes per hour (ACH) or the use of an air purifier were required in the seating areas of dine-in catering premises [18].

Since the pandemic began in 2020, Hong Kong had implemented various social distancing measures which varied on the outbreak situations (Fig. S1; [16,17,19,23]). At the time of the investigated outbreak, no dine-in eating with more than four people per table is permitted, which was implemented on February 18, 2021, just before the outbreak. A 1.5 m distance between tables or use of partitions was required

which had been in place since 2020. Mask-wearing remained mandatory in public places except while eating or drinking, and catering staff were subject to regular RT-PCR testing every 14 days.

In this study, we aim to investigate the outbreak with a three-zone airflow model, the Wells–Riley equation, field measurement, and whole-genome sequencing. We estimated the airflow rates and air distribution in the three zones using the field measurement data. We hypothesise that the long-range airborne route is predominant in this outbreak. The outbreak is characterized by a lack of secondary infection among patrons in Zones A and C and the concomitant high attack rate in the central Zone B. This characteristic will be used, together with the estimated ventilation data, to provide us with a reliable estimate of the infectious quanta generation rate.

2. Methods

2.1. Outbreak data

During lunchtime on 19 February 2021, a major outbreak of COVID-19 occurred at a restaurant (hereafter, Restaurant M) in Kowloon, Hong Kong. The index case was identified as an older male cleaner (age: 72 years) who was primarily responsible for cleaning tables and collecting dishes. The cleaner had tested negative for COVID-19 via the real-time reverse transcription-polymerase chain reaction analysis (RT-PCR) of throat swabs on 14 February and had not worked in the restaurant between 16 and 18 February. The throat swab sampling was conducted by the Department of Health of the Government of the Hong Kong Special Administrative Region (HKSAR), while the RT-PCR testing was performed by government-certificated laboratories in Hong Kong. The index case began coughing on 18 February and developed a fever in the afternoon of February 19 after he worked at the restaurant between 11 a.m. and 3 p.m.

On 25 February 2021, the Centre for Health Protection (CHP) of HKSAR government found that eight of 11 confirmed daily positive cases had lunch at Restaurant M on 18 and 19 February, while the remaining three cases involved restaurant staff. Subsequently, the CHP asked people who had visited the restaurant between noon and 3 p.m. on 19 February 19 to participate in an investigation, and required any person who visited the restaurant between 18 and 24 February to undergo compulsory testing by 26 February. In total, 52 confirmed cases were identified, including 22 patrons, 10 restaurant staff and 20 people who were close contacts of these patrons and staff. Detailed information about each confirmed case is available in Table S1 (Supplementary S1).

Among the 76 patrons who had lunch at the restaurant on 19 February, 21 cases, including 14 symptomatic and seven asymptomatic cases, were confirmed by RT-PCR analysis of throat swabs. Additionally, one of the 22 infected patrons was a family member of the index case who visited the restaurant on 18 February. Among the 19 staff (11 waiters and eight kitchen staff) who worked in the restaurant on 19 February, 10 cases were confirmed by RT-PCR analysis of throat swabs, and all infected staff were symptomatic. The epidemic curve of the outbreak as part of entire pandemic in Hong Kong (Fig. S1) is shown in Fig. 1. The peak onset date for secondary cases (patrons or staff) was 22 February, which is consistent with published data on the COVID-19 incubation period [12,15]. The whole-genome sequencing and phylogenetic analysis methods are described in Cheng et al. [10].

The restaurant was designed to accommodate 119 patrons and 20 staff and has a total floor area of 175.3 m², including two VIP rooms. According to the Hong Kong Public Health and Municipal Services Or-

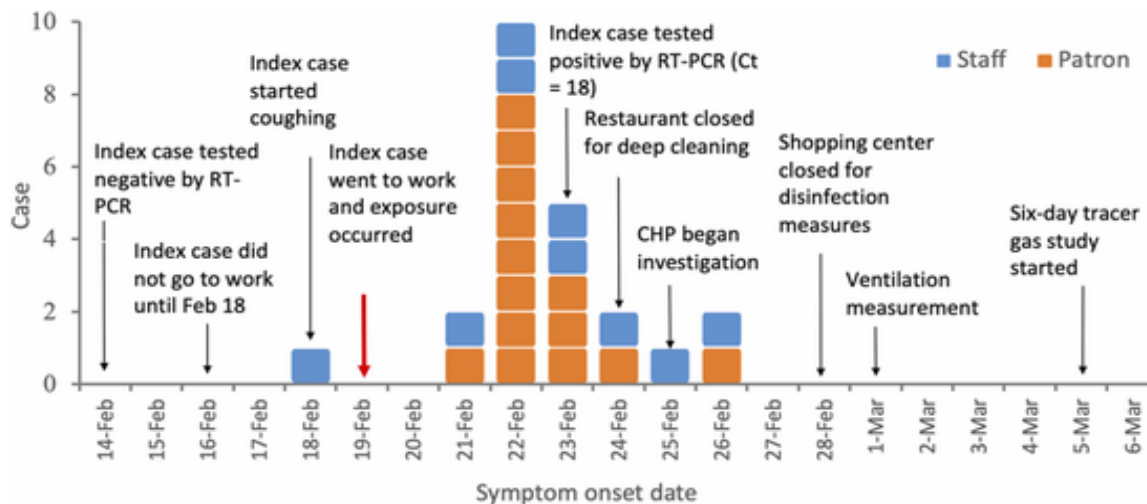


Fig. 1. The epidemic curve of the Restaurant M outbreak and the timeline of relevant involved events.

dinance [7], a minimum outdoor air flow rate of $17 \text{ m}^3/\text{h}$ (4.7 L/s) per person is required. Therefore, an outdoor air flow rate of at least 559 L/s is needed in both the design and operation of this restaurant, based on the number of patrons.

The seating areas are located on two floors: the first floor (Zone A) has an entrance from the open area of the shopping arcade, and the lower ground floor (Zones B and C) has exterior walls. The seating areas are separated into three zones. Zone A is open to the shopping arcade. The entire restaurant has only one air exhaust, located in the kitchen. The kitchen draws air from Zone A, which in turn draws air from the shopping arcade via the open entrance and from Zone B via a staircase. On the lower floor, Zone B is connected to two VIP rooms and a passage room, which were unlikely to have been in use at the time, as indicated by the absence of secondary infections. All 21 known secondary patron infections occurred in Zone B. The exact tables where only 20 secondary infected patrons sat are known, but their exact seats remain unknown. Accordingly, the infected seats were randomly assigned to each infected table, as shown in Fig. 2a.

The restaurant is equipped with 21 FCUs, 19 of which are installed in the seating areas (Fig. 2b). Our onsite inspection found that seven FCUs in the seating areas supply outdoor air (shown in blue), and the remaining FCUs only recirculate room air for cooling. As the only exhaust is located in the kitchen, excess air from Zone B flows into Zone A via a staircase, and the mixed air in Zone A is then exhausted into the kitchen. This airflow pattern means that contaminated air from Zone B also poses an exposure risk for patrons in Zone A.

All of the restaurant staff ate lunch together in Zone B, before the restaurant was opened to patrons, and then worked in their respective areas for the rest of the day. The elderly cleaner was responsible for cleaning tables and collecting dishes in Zones B and C after the patrons had finished their meals and spent most of his time in the cleaner room or occasionally in the bar area. The CHP collected 48 environmental samples from various places in the restaurant on 1 March, including from the handle of trolley, food tables, sink taps, tables beside sink and inner surface of sink drain pipe in the kitchen (15 samples); sink tap, handles of water heaters, table beside sink and inner surface of sink drain pipe in tea station in the first floor (4 samples); sink taps, tables beside sink, bar counter top, U trap of sink and inner surface of sink drain pipe in the water bar (7 samples); surfaces of trolley, handle of water heater, sink taps, table beside sink and inner surface of sink drain pipe in the cleaner room (7 samples); a cabinet surface in Zone B (one sample); and FCU filters, fresh air louvers and return air louvers in all areas (14 samples).

2.2. Experimental study

Prior to our field measurements, the Electrical and Mechanical Services Department (EMSD) of the HKSAR inspected the restaurant's ventilation system on 1 March 2021. The rates of outdoor air flow to FCUs F6, F13, F19 and F20 were measured using an anemometer. Due to data loss during the outbreak, the only real-time data from the primary air handling unit (PAU) to the restaurant and other shops in the shopping centre on 1 and 3 March 2021 were recorded and provided by the Building Management System (BMS). Both the BMS data and the data obtained from inspection measurements were used in our analysis.

Our field measurements were conducted from 5 to 10 March 2021, while the shopping centre was closed for quarantine. Tables and chairs were arranged based on the descriptions provided by restaurant staff to replicate the setup during the outbreak. Two to four simple thermal mannequins, each equipped with an 80-W electrical bulb encased in a hollow stainless-steel shell to simulate body heat dissipation, were placed at each table in accordance with the Hong Kong restriction mandating a maximum of four persons per dine-in table at that time. During the tests, all FCUs and kitchen exhaust fans were operational. The temperature and velocity of the supply air, the geometry of supply air inlets at each FCU and the velocity of the outdoor supply air at FCUs 6, 11 and 14 were measured. Additionally, we also placed five temperature/humidity sensors (EL-USB-2, Lascar Electronics, Wiltshire, UK) and four weather stations (HOBO U30 NRC, Onset, Bourne, Massachusetts, USA) inside and outside the restaurant. The opening and closing status of the doors and windows were adapted to the specific experimental needs. The entire geometry of the restaurant was captured using a 3D scanner (PX-80, Paracosm, USA).

Three types of field experiments were conducted: the air change rate, dispersion and bidirectional flow experiments. In this paper, *ventilation flowrate* into a zone refers to the supplied outdoor air flow rate by the PAU and infiltration through the envelope; *equivalent ventilation flowrate* is the sum of outdoor air (ventilation air) and 'virus-free' air from neighbouring spaces; and *total dilution air flowrate* is the sum of the equivalent ventilation flowrate and the equivalent dilution air flowrates due to aerosol settling, filter filtration and virus deactivation. The air change rate experiments primarily aim to measure ventilation flowrate or equivalent ventilation flowrate, while both the dispersion and bidirectional flow experiments focus on the total dilution air flowrate together. Note that the equivalent ventilation flowrate is conceptually ambiguous, as for Zone A, the airflow from Zone B may not be

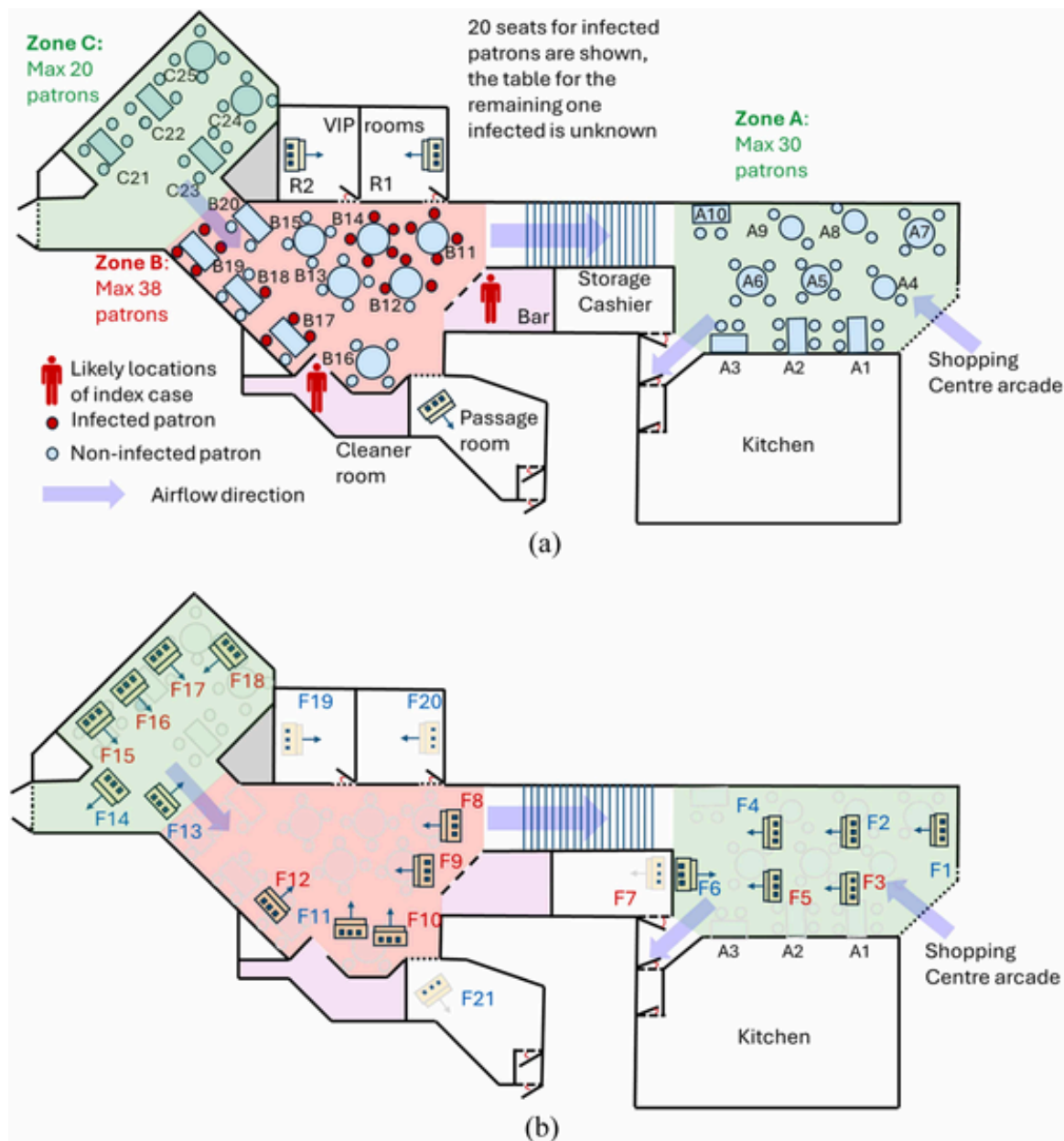


Fig. 2. The infection venue. (a) The locations of all 25 tables in the artificially separated three zones, the numbers of secondary infections at each table and the likely locations of the index case are shown. The exact seats of the secondary infection cases at each table remain unknown. (b) The locations of the fan coil units (FCUs), with net airflow directions between the three zones shown in light blue arrows. There are 19 fan coil units directly located in the seating areas of the restaurant.

virus-free for quanta mitigation analysis; we only assume that it is virus-free at the time of field measurements.

In the air change rate experiments, we aimed to measure the air change rate due to equivalent ventilation flowrate in Zone A, Zone BC (Zones B and C were combined for measurement purposes), VIP Rooms R1 and R2, the passage room and the kitchen. We released sulfur hexafluoride (SF_6) into each area through a pipe with an 8-mm inner diameter at a flow rate of 1.5 m/s and ceased the release once the SF_6 concentration reached a sufficiently high level. Four high-powered fans were used to mix the air within each measurement area. SF_6 concentrations were monitored at multiple points at a height of 1.1 m using a 24-channel multipoint sampler and a photoacoustic gas monitor (Innova 1409 and 1412i, LumaSense Technologies, Hovedstaden, Denmark), as well as a six-channel multipoint sampler and a photoacoustic gas moni-

tor (Innova 1403 and 1512, LumaSense Technologies). The number of monitoring points was selected based on the geometry of each zone, while the duration of monitoring was determined by the estimated air change rate in each zone (see Table S2). The air change rate experiments were repeated two or three times per zone.

In the dispersion experiments, we released SF_6 and fine particles at a height of 1.1 m from specific locations: the cleaner room, the water bar and a mobile release source in Zone BC. Therefore, these are referred to as the cleaner-room dispersion, water-bar dispersion and well-mixed dispersion experiments, respectively. SF_6 was introduced from a gas cylinder through a pipe with an 8-mm inner diameter at a flow rate of 1.5 m/s, while fine particles were generated using a self-made fine particle generator at a flow rate of 15 L/s. The particle generator involved burning incense sticks and an exhaust fan, and the test data indicated

that it primarily produced PM1 particles. We compared differences in the removal of tracer gas and fine particles. SF₆ and fine particle concentrations were monitored at a height of 1.1 m at several points using a 24-channel multipoint sampler and a photoacoustic gas monitor (Innova 1409 and 1412i, respectively), a six-channel multipoint sampler and a photoacoustic gas monitor (Innova 1403 and 1512, respectively), two optical particle sizers (OPS 3330, TSI Inc., Shoreview, Minnesota, USA), two Dust-Track DRX aerosol monitors (desktop model 8533 and handheld model 8534, TSI Inc.) and an aerodynamic particle sizer (APS 3321, TSI Inc.) (see detailed measurement points Table S2). Four high-power fans were operated only during the source release periods of the well-mixed dispersion experiments.

Simple smoke tests confirmed the predominant airflow from Zone B to Zone A. The cleaner had mainly worked in Zones B and C. In the bidirectional flow experiment, six air flowrates in two seating areas (Zone A and Zone BC) were measured using the two-tracer and two-zone decay method. We simultaneously released SF₆ into Zone A and carbon dioxide (CO₂) into Zone BC from two gas cylinders for 30 mins to achieve high tracer concentrations in the respective zones. The door to the shopping arcade in Zone A was closed during the release phase and opened after the release stopped. Four high-power fans were used throughout the experiment to mix the air in Zones A and BC. The SF₆ and CO₂ concentrations were monitored at two points 1.1-m-height points in Zone A, one 1.1-m-height point in Zone BC and four points at the interface between the staircase and the two seating areas (two points located 0.5 m from the ceiling and two points located 0.5 m from the floor). Monitoring was done using a 24-channel multipoint sampler and photoacoustic gas monitor (Innova 1409 and 1412i, respectively) and a six-channel multipoint sampler and photoacoustic gas monitor (Innova 1403 and 1512, respectively) (Fig. S2). All thermal mannequins in Zone BC were turned on. The experiments were repeated twice. In the first test, the staircase was sealed with a polyvinyl chloride (PVC) sheet during the release phase, which was removed afterwards. In the remaining two tests, the staircase was not sealed with a PVC sheet during the release phase.

2.3. Methods of airflow rate and air distribution estimation in the three zones

In the air change rate experiments, the SF₆ concentration in the tested zone was significantly higher than in other zones during a considerable tracer decay phase. This allowed us to approximate the airflow from other zones to the tested zone as tracer-free airflow. Consequently, the slope of the linear regression of the logarithm of the SF₆ concentration over time was used to determine the equivalent ventilation air change rate [35]. Additionally, we assumed that the air in the tested zone was well mixed.

In the dispersion experiments, the SF₆ and fine particle concentrations were used in two ways. First, we estimated the normalised concentration at each tested table, using tracer data collected during the release phase, and further calculated the normalised exposure based on the normalised concentration and exposure duration. This allowed us to compare the normalised concentration and exposure with the attack rate at each table (see results in Fig. S4 and Table S5, Supplementary S3). Second, we estimated the particle removal rate and SF₆ removal rate by using their respective concentration profiles after the release stopped [24,3,9]. The difference between the particle and SF₆ removal rates is attributed to the particle deposition rate and filtration by the FCUs (See results in Fig. S6, Supplementary S4). Additionally, we estimated the recirculation flow rate of the FCUs by assuming a base deposition rate of 0.3 for PM1 particles and a filtration efficiency of 9.5% for PM1 (see details in Supplementary S7).

In the bidirectional experiments, we used two-zone and two-tracer mass balance modelling to estimate six airflow rates in Zone A and Zone BC (Fig. S7; [28]). Due to the nonlinear relationship between the math-

ematical model and these six unknown airflow rates, an analytical solution was not possible. Therefore, we used an iterative, nonlinear, least-squares minimisation method to obtain a numerical solution based on the SF₆ and CO₂ concentrations in Zone A and BC [14]. The detailed methods can be found in Supplementary S5.1.

2.4. Three-zone airflow model for modelling infection risk

The Wells–Riley model [21,34] is used to evaluate the infection risk P_i in one of the three zones:

$$P_i = \frac{N_i}{N_{\sigma,i}} = 1 - e^{-C_i q_{in} \Delta t} \quad (1)$$

where $C_i = \frac{1}{\Delta t} \int_t^{t+\Delta t} C_i(t) dt$ is the average quanta concentration in the i^{th} zone (quanta/m³), and $q_{in} = 0.20$ L/s is the inhalation rate associated with light activity during lunch [40]. Δt is the exposure time (s): the average lunch time of the 20 infected patrons was 3900 s, similar to the range of 3600–4200 s reported in Zhang et al. [46].

As the cleaner mainly worked in the cleaner room and was responsible for cleaning tables in Zones B and C, we first assumed a quanta emission source in the cleaner room as a part of Zone B.

We assumed that each zone was well mixed (i.e. had a uniform quanta concentration). Unfortunately, we did not initially address the lack of infection in Zone C and did not measure exchange airflows between Zones B and C during the bidirectional flow experiments. However, airflow from Zone C to Zone B is expected due to the net air supply into Zone C via two outdoor FCUs and the building envelope. Some airflow from Zone B to C is also possible, depending on the air temperature difference between the two zones. The airflow rates q_{23} and q_{32} were tried with different values according to the net air supply into Zone C to reproduce the unique infection feature. The three zones are numbered as 1 for Zone A, 2 for Zone B and 3 for Zone C; 0 represents outdoor air.

$$V_1 \frac{dC_1(t)}{dt} = q_{21}C_2(t) - (q_{10} + q_{12} + (\lambda_{dep} + \lambda_{dea})V_1 + \eta q_{FCU,1})C_1(t) \quad (2)$$

$$V_2 \frac{dC_2(t)}{dt} = q_{12}C_1(t) + q_{32}C_3(t) - (q_{20} + q_{21} + q_{23} + (\lambda_{dep} + \lambda_{dea})V_2 + \eta) \quad (3)$$

$$V_3 \frac{dC_3(t)}{dt} = q_{23}C_2(t) - (q_{30} + q_{32} + (\lambda_{dep} + \lambda_{dea})V_3 + \eta q_{FCU,3})C_3(t) \quad (4)$$

where $\lambda_{dep} = 0.3$ is the deposition rate (h⁻¹) [11,39]; $\lambda_{inc} = 0.63$ is the deactivation rate (h⁻¹) [13,41]; \dot{Q} is the quanta emission rate of the index case (quanta/h); and q_{ij} is the air flowrate from zone i to zone j . This system of three linear equations can be easily solved. As the infected patrons did not arrive until around 1 pm, the index case would have been in the restaurant for nearly 2 h prior, allowing a steady-state solution for the quanta concentration to be reached in the three zones. This steady-state quanta concentration can be used in the Wells–Riley Eq. (1).

3. Result

3.1. The spatial seat distribution of secondary infected cases was non-uniform

A striking feature of the outbreak is that all secondary infected patrons were seated in Zone B. No secondary infections were found among patrons in Zones A and C. The 21 infected patrons had lunch between 1 and 3 p.m. on 19 February, according to contact tracing by CHP (Table S1). There were 76 patrons present during the lunch time slot. However, except for tables with secondary infections, the tables where each of the 76 patrons sat remained unknown (Fig. 2a). In our analyses, we

assumed a proportional distribution based on the available tables, i.e. 26 in Zone A, 33 in Zone B and 17 in Zone C. At the time, each table was limited to at most four patrons. With a maximum capacity of 88 seats at the time, due to the four-seat policy, and 76 patrons, 86.4% of the seats were likely to have been occupied at the peak time. It is likely that all tables were occupied, with some tables having fewer than four patrons. Note that B14 had five patrons. Given this assumption, the attack rate in Zone B is as high as 63.6%, while the attack rates in the other two zones are zero. As the maximum number of patrons in Zone B was 38, the lowest possible attack rate is 55.3%.

It is unknown when and where the 10 infected staff (four kitchen staff and six waiters) were exposed, but their joint lunch in Zone B on 19 February is one of the suspected settings. The attack rates among kitchen staff and waiters are similar at 50% and 54.5%, respectively, suggesting that both groups might have become infected when they were together and had a similar exposure time, i.e. their joint lunch time. The sample size of both kitchen staff and waiters is small. Phylogenetic analysis of the infected cases (both staff and patrons) showed clustering together, suggestive of transmission in the restaurant by a single source (Fig. S10).

Three surface samples were found to be positive, including the inner surface of the sink's down pipe in the cleaner room. The index case stayed in the cleaner room most of the time. Multiple routes might explain the positive sample collected at the sink, including utensils that had been contaminated by the index case. The second positive sample was the handle of the trolley used by the index case. It is also possible that the index case did not wear a mask during some of the time when he was in the cleaner room and out of sight of others.

The third positive sample was collected from the filter of FCU 15 (see Fig. 2b for its location), which is located in Zone C, suggesting either that contaminated air had escaped from Zone B to Zone C, or that virus particles were released during the short period when the index case worked in Zone C.

3.2. Estimating airflow distribution and equivalent ventilation rates in Zones A, B and C

The exponential decay of the SF₆ concentrations in each zone indicates that the air change rates estimated using the single tracer-gas method are reliable (Fig. S3). Under the default experimental settings, i.e. the main entrance between Zone A and the shopping arcade and the staircase between Zones A and B remained open and the doors and windows of VIP rooms R1 and R2, the passage room and Zone C remained closed, the average equivalent ventilation air change rates were estimated as follows: 21.7 h⁻¹ in Zone A, 2.99 h⁻¹ in Zone BC, 10.1 h⁻¹ in VIP rooms R1 and R2, 8.2 h⁻¹ in the passage room and 55.7 h⁻¹ in the kitchen. Accordingly, the equivalent ventilation flowrates were estimated to be 1008 L/s in Zone A, 326 L/s in Zone BC, 164 L/s in VIP rooms R1 and R2, 66 L/s in the passage room and 2446 L/s in the kitchen (Table S3). The outdoor airflow rate through the three FCUs (F11, F13 and F14) in Zone BC was calculated to be 96 L/s, based on the difference in equivalent ventilation flowrates between Zone BC and VIP rooms R1 and R2 and the passage room. Assuming an identical outdoor airflow rate for each FCU (F11, F13 and F14), the rate for each FCU would be 32 L/s, which is consistent with the air-duct measurements of 30.8 L/s obtained on 5–10 March. Other testing scenarios besides the default settings are available in Supplementary S2.

In VIP rooms R1 and R2 and Zones B and C, the ratio of outdoor air flow rates between our field tests and EMSD's tests is approximately 1.6. However, in Zone A, this ratio is about 2.4, based only on our air-duct measurement of 113 L/s for FCU F6 and EMSD's measurement of 48 L/s. As both our single tracer-gas method and bidirectional flow method for Zone A included the airflow from the shopping arcade, further validation of the ratio of 2.4 in this zone was not possible. This ratio may be attributable to measurement errors when using the

anemometer to measure airflow speed across the air-duct plane. Therefore, in the following analysis, we use the ratio of 1.6 obtained from VIP rooms R1 and R2 and Zones B and C to quantify the difference in outdoor airflow rates between our test period and the EMSD test period (Table S4), and to estimate the three-zone exchange airflow rates under the EMSD test conditions (Table 1).

In the bidirectional flow experiments, the two-zone and two-tracer model successfully reproduced the measured data (Fig. S9). Fig. 3a shows the measured and predicted of the two tracer gas concentrations along the decay curve in the first test trial with results in other two tests trails shown in Fig. S9. The normalised prediction errors are relatively small (Fig. 3b), indicating that the estimation of the unknown air flow rates in the three bidirectional experiments was relatively accurate. The equivalent rates of 'outdoor air' air flow to Zones A and BC (q_{01} and q_{02}) were estimated to be 688 L/s and 381 L/s, respectively (Table S6), lower than the respective rates of 936 L/s and 407 L/s estimated using the single tracer-gas method. This discrepancy is attributable to the exchange airflow rates: $q_{21} = 240$ L/s from Zone B to A and $q_{12} = 26$ L/s from Zone A to B. The exchange airflow in each zone also played a diluting role in the other zone. Hence, the equivalent ventilation rate of 936 L/s in Zone A, determined using the single tracer-gas method, corresponds to $q_{01} + q_{21} = 928$ L/s as determined using the bidirectional flow method. The equivalent ventilation rate of 407 L/s in Zone BC, determined using the single tracer-gas method, corresponds to $q_{02} + q_{12} = 407$ L/s as determined using the bidirectional flow method. Hence, the bidirectional flow method effectively determined the exchange airflows between the two zones, whereas the single tracer-gas method only identified the total in-flow rate (e.g. $q_{01} + q_{21}$) or total out-flow rate (e.g. $q_{10} + q_{12}$) in each zone.

Furthermore, we compared the equivalent ventilation rates determined in three bidirectional experiments with those determined in the air change rate experiments. In Zone A, the average equivalent ventilation rate was 928 L/s (standard deviation: 124 L/s) in the three bidirectional experiments, compared with an average equivalent ventilation rate of 1008 L/s (standard deviation: 118 L/s) in several air change rate experiments. Similarly, in Zone BC, the average equivalent ventilation rate was 407 L/s (standard deviation: 10 L/s) in the three bidirectional experiments and 326 L/s (standard deviation: 30 L/s) in several air change rate experiments. These results also indicate that the test conditions were essentially the same across the experimental days. More details are available in Supplementary S5.2.

3.3. Explanation for heterogenous infection distribution in three connected zones

Insufficient dilution explains the high attack rate in Zone B, while good dilution and a favourable air flow direction respectively explains the lack of infection in Zones A and C. The monitoring data indicate that the dilution conditions were poorer in the three zones on 1 March 2021 than during 5–10 March. The PAU, which is responsible for supplying outdoor air to the restaurant and other shops, is monitored by the building management system (BMS). The BMS PAU data between 18 and 23 February 2021 were not made available. According to a site inspection by EMSD, the PAU was operated at 510 L/s on 1 March 2021 but at 1700 L/s on 3 March 2021. During the field measurements between 5 and 10 March, the outdoor air supply rates were higher than those measured by EMSD on 1 March. Our best estimates of the air flow rates for the two possible scenarios (1 March and 5–10 March) are summarised in Table 1. There are significant differences in the outdoor air flowrates between the two scenarios. The total dilution flowrates are dominated by the filtration effects of the FCUs instead of the original supply outdoor air. For the 1 March dilution scenario, if the FCUs operated at their designed flow rates, the equivalent dilution flowrates per patron are 40.3 L/s in Zone A and 45.8 L/s in Zone C, with a lower rate of 19.4 L/s in Zone B, where infection transmission occurred. For the

Table 1

Dilution flowrates and exchange flows in the three-zone restaurant. The flowrate q_{ij} refers to the flowrate from zone i to zone j (0 for outdoor air, 1 for Zone A, 2 for Zone B and 3 for Zone C).

Flowrate (L/s)	Based on monitoring data from 1 March	Based on monitoring data from 5–10 March	Notes
q_{01}	430	688	These are the total outdoor air flowrates into each zone. q_{01} also includes the airflow rate from the shopping arcade. q_{02} only includes the outdoor airflow from the primary air handling unit, while q_{03} also includes the infiltration airflow via the building envelope.
q_{02}	81	130	
q_{03}	157	251	
q_{10}	564	902	The air flow from Zone BC to outdoors was estimated in bidirectional experiments; here, it is assumed to have leaked through the C envelope only after the site observation.
q_{20}	0	0	
q_{30}	104	167	
q_{12}	16	26	EMSD did not measure the exchange flow among the three zones, which was estimated using our two-tracer results.
q_{21}	150	240	
q_{23}	50*	50*	
q_{32}	103 (84/1.6 + q_{23})*	134 (84 + q_{23})*	
$q_{dep+inc,01}$	43.2		A constant 0.3 h^{-1} for aerosol settling and 0.63 h^{-1} for virus deactivation is assumed.
$q_{dep+inc,02}$	61.2		
$q_{dep+inc,03}$	32.8		
$q_{FCU,1}$ ($\eta q_{FCU,1}$)	2638 (575.1)	2521 (549.6)	The filtration efficiency of the FCUs for PM2.5 is 21.8%[6]. The FCUs were operated at the designed nominal flowrate.
$q_{FCU,2}$ ($\eta q_{FCU,2}$)	2279 (496.8)	2230 (486.1)	
$q_{FCU,3}$ ($\eta q_{FCU,3}$)	2703 (589.3)	2627 (572.7)	
Zone A (1), total dilution rate $q_{T,1}$ ($q_{t,1}$)	1048.3 (40.3)	1280.8 (49.3)	
Zone B (2), total dilution rate $q_{T,2}$ ($q_{t,2}$)	639 (19.4)	677.3 (20.5)	
Zone C (3), total dilution rate $q_{T,3}$ ($q_{t,3}$)	779.1 (45.8)	856.5 (50.4)	
$q_{FCU,1}$ ($\eta q_{FCU,1}$)	1082 (235.8)	1034 (225.3)	Same as above; the FCUs have a filtration efficiency for PM2.5 of 21.8%[6] but were operated at the estimated 41% of the designed flowrate (Supplementary S7).
$q_{FCU,2}$ ($\eta q_{FCU,2}$)	934 (203.7)	914 (199.3)	
$q_{FCU,3}$ ($\eta q_{FCU,3}$)	1108 (241.5)	1077 (234.8)	
Zone A (1), total dilution rate $q_{T,1}$ ($q_{t,1}$)	709 (27.3)	956.5 (36.8)	
Zone B (2), total dilution rate $q_{T,2}$ ($q_{t,2}$)	345.9 (10.5)	390.5 (11.8)	
Zone C (3), total dilution rate $q_{T,3}$ ($q_{t,3}$)	431.3 (25.4)	518.6 (30.5)	

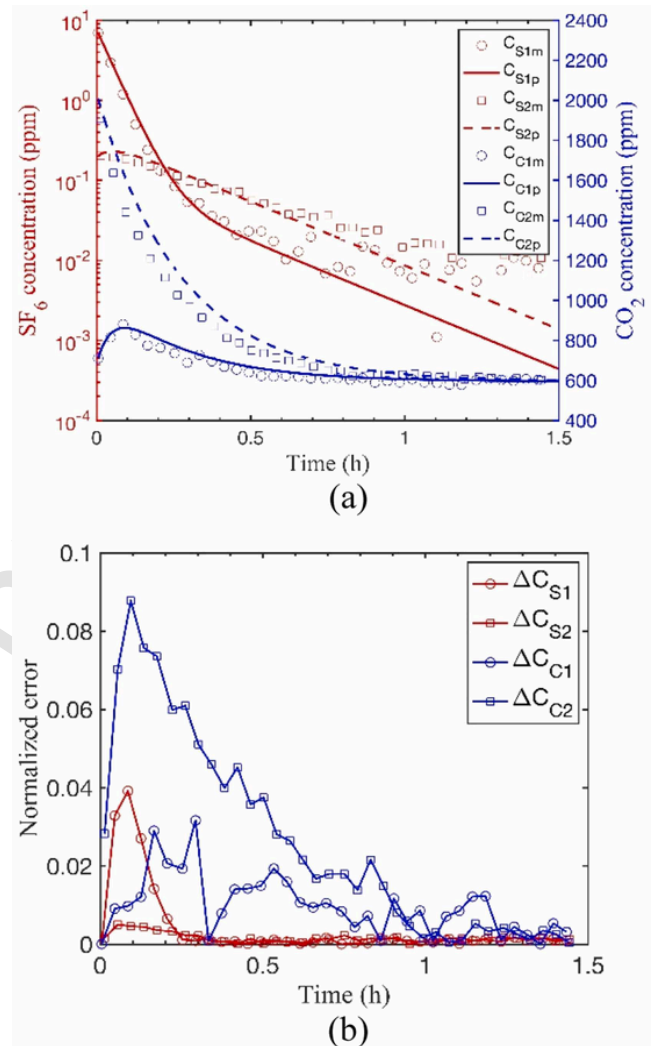


Fig. 3. Comparison of predicted tracer gas concentrations using the measured air flow rates and the measured tracer gas concentrations. (a) SF₆ and CO₂ concentrations in the first test trial; (b) normalised prediction errors of SF₆ and CO₂ in the first test trial. ‘m’ and ‘p’ in the symbols of ‘C_{S1m}’ or ‘C_{S1p}’ represent the measured and predicted values, respectively. The normalised prediction error is defined as the difference between the predicted and measured values at a given time, divided by the maximum measured value throughout the measurement period.

5–10 March dilution scenario, the equivalent dilution flowrates per patron were 49.3 L/s in Zone A, 20.5 L/s in Zone B and 50.4 L/s in Zone C. Additionally, when the FCUs operated at 41% of their designed flow rates (see Supplementary S7 for the derivation of this operating percentage), the equivalent dilution flow rates changed as detailed in Table 1.

The three-zone model was used to estimate quanta exposure. The quanta generation rates were estimated to produce lowest and highest attack rates of 55.3% and 63.6%, respectively, in Zone B. The corresponding infection risks in Zone A and Zone C were also estimated. For the likely number of patrons, the attack rate would need to be less than 3.85% in Zone A and less than 5.88% in Zone C to avoid a single secondary infection. The FCUs filter fine particles, and the filtration efficiency for PM2.5 was measured as 20% by Li et al. (2022) and 21.8% by Cao et al. [6]. The latter value of 21.8% was adopted for our study. Additionally, our measurements from 5–10 March probably were measured under a ‘modified’ condition, as high and unacceptable levels of

noise from the operation of the FCUs could be heard in the restaurant. Table 2 shows that under the 'modified' condition from 5–10 March, in only two of the tested conditions with the FCUs operated at the designed flow rates and an appropriate exchange airflow between Zone B and Zone C, the respective predicted quanta generation rates of 3108 quanta/h and 3688 quanta/h resulted in an acceptable range of attack rates in the two non-infection zones, and the predicted quanta generation rate was the highest among all acceptable quanta generation rates (highlighted in bold green and red). Table 2.

As the exchange airflows between Zone B and Zone C were not measured, we must make an assumption. We first assumed a small exchange air flowrate of $q_{32} = 50$ L/s and then identified a larger value of 118 L/s, which provides the highest acceptable attack rate in Zone C (5.8%). The FCUs were found to operate at 41% of the designed flow rate (Supplementary S7). We thus predicted quanta generation rates of 1724 and 1968 quanta/h. At a small exchange flow rate of 50 L/s, the escape of expired viruses from Zone B to C might be too small to explain the positive sample collected from the FCU 15 filter. Both the quanta generation rates of 1724 and 1968 quanta/h would result in sufficiently small attack rates and no secondary infection in Zones A and C, as well as the correct attack rate in Zone B. As escape from Zone B to C was greater in the latter case with an exchange flow rate of 118 L/s, a generation rate of 1968 quanta/h is probably the correct value. Other relevant scenarios are detailed in Tables S7 and S8 (Supplementary S6).

Additionally, a filtration efficiency of 10% and an FCU operation flow rate ratio of unity were also tested, and the resulted quanta generation rates are listed in Table 2 for reference only. These predicted values are not considered to be reliable as we lack data support for the chosen filtration efficiency or FCU operation flow rate ratio.

4. Discussion

4.1. How large can the maximum quanta generation rate be?

Both epidemiological investigations and whole-genome sequencing revealed that the investigated outbreak was due to a single source, namely a cleaner. The Ct value of the index case was 18 when tested on February 23, indicating a high viral load. The unique feature of the studied outbreak is the co-existence of both infection and non-infection in three connected zones in a single restaurant, i.e. the occurrence of secondary infections only in one seating zone, with an absence of infection in the two other connected zones. This scenario leads us to ask why the transport of quanta-contaminated air from the infection zone did not cause infection in the two other zones. The three connected zones are separated by both physical and non-physical barriers. Zones A and B

are separated by a long staircase, with dominant exchange airflow from Zones B to A as confirmed by our field measurements. While there were no physical barriers between Zones B and C, the airflow generated by fan coil unit F13, likely creates some barrier effect. There should be some airflow between Zones B and C. At the time of our field study, the project team did not realise the importance of this unique feature; consequently, the exchange airflows between Zones B and C were not directly measured but estimated.

After considering the filtration contribution of the FCUs, the total dilution air flowrates become significantly high even in the infected Zone B, where the total dilution air flowrate could still reach approximately 20 L/s per person. This is much higher than the typical values reported for outbreaks in the literature: 5.5 L/s per person in a courtroom [42], 7.6 L/s per person in a restaurant [27] and 2.1 and 3.5 L/s per person in two buses [31]. At a constant attack rate, a high equivalent dilution air flowrate implies a large quanta generation rate.

Our simple three-zone model estimate suggests that the likely quanta generation rate was 1968 quanta/h, which may be the highest quanta generation rate observed to date; to our best knowledge, it is higher than any reported value in the literature [27,29,31,42]. Due to the predominant airflows from Zone C to B and the large equivalent dilution air flow rate in Zone C, the quanta concentration was relatively low in Zone C. However, according to even our simple three-zone model, some quanta-contaminated air escaped from Zone B to C. This result is supported by the positive SARS-CoV-2 swab sample collected from the filter of FCU 15 in Zone C. However, the fact that the index case might have briefly moved to Zone C to clean tables after lunch could also explain the existence of this positive swab sample.

The observed high quanta generation rate is also supported by the positive sample collected from the sink in the cleaner room, where the index case spent most of his time during the exposure period. Probably, the index case removed his face mask for some of his time in the cleaner room, as he was away from the patrons. However, due to pandemic policy, the index case must have worn his mask while cleaning tables in Zone B or Zone C.

Due to the lack of behavioural data for the index case and the patrons, we cannot completely rule out a possible role of short-range transmission between the index case and any infected patrons. However, mask wearing was compulsory for restaurant staff at the time of the outbreak in Hong Kong. It was very likely that the index case wore his mask while he was in the seating area. The short-range exposure effect is likely negligible when wearing mask at a physical distance greater than 0.3 m [45]. However, we cannot completely rule out the possibility of short-range airborne transmission. Particularly, there

Table 2

Estimated infection risks in the three zones under different airflow scenarios. For the probable number of patrons, the attack rate should be less than 3.85% in Zone A and 5.88% in Zone C to avoid a single secondary infection in these zones. The acceptable attack rates are highlighted in bold green font, and the corresponding quanta generation rates are also highlighted in bold green font when the attack rates in both Zones A and C are sufficiently low for the EMSD setting and in bold red font for our measurement setting.

Scenario description			EMSD setting (1 March 2021)			Our measurement setting (5–10 March 2021)		
Filtration efficiency η (%)	FCU operation flow rate ratio [#]	Exchange flow q_{23} (L/s)	Quanta emission rate (quanta/h)	Attack rate of Zone A (%)	Attack rate of Zone C (%)	Quanta emission rate (quanta/h)	Attack rate of Zone A (%)	Attack rate of Zone C (%)
21.8	0.41	50	1724 (2162)*	3.8 (4.8)	2.3 (2.9)	2040 (2562)	4.4 (5.5)	2.0 (2.4)
21.8	0.41	118	1968 ^{&} (2470)	3.8 (4.8)	4.7 (5.8)	2286 (2870)	4.4 (5.5)	4.1 (5.1)
21.8	1	50	2814 (3532)	2.8 (3.5)	1.3 (1.7)	3108 (3902)	3.5 (4.3)	1.2 (1.5)
21.8	1	210	3394 (4260)	2.8 (3.5)	4.6 (5.8)	3688 (4630)	3.5 (4.3)	4.3 (5.4)
10	0.41	50	1312 (1648)	4.5 (5.6)	3.1 (3.9)	1638 (2056)	4.9 (6.1)	2.5 (3.1)
10	0.41	118	1556 (1952)	4.5 (5.6)	6.1 (7.6)	1882 (2362)	4.9 (6.1)	5.1 (6.3)
10	0.41	236	1972 (2474)	4.5 (5.6)	9.4 (11.6)	2300 (2886)	4.9 (6.1)	8.1 (10.0)

[#]The fan coil unit (FCU) operation flow rate ratio of 0.41 is the fraction of the actual recirculation flow rate to the designed flow rate of an FCU, which is determined in Supplementary S7.

* Values outside of brackets are based on the attack rate of 55.3% in Zone B, and values inside of brackets are based on the attack rate of 63.6% in Zone B.

[&] The most reliable predicted quanta generation rate is 1968 quanta/h.

might be a leakage flow at mask perimeters [36,37], which can potentially lead to short-range airborne transmission.

Cheng et al. [10] estimated a quanta generation rate of 557.7 quanta/h for the same outbreak, assuming that the entire restaurant was a single well-mixed zone. In contrast, our three-zone model accounts for spatial non-uniformity of exposure, resulting in a much greater quanta generation rate of 1968 quanta/h. It is crucial to consider spatial non-uniformity when estimating quanta generation rates. The detailed air distribution and associated dispersion of expired droplets could have been studied by using computational fluid dynamics, which also required detailed input of geometrical and ventilation parameters at boundaries, which are not all available. The distribution of air flows would impact on the distribution of expired droplets in the space [20,25,27,32]. Future studies of such a complex geometry will need special care in obtaining all required data for simulations.

Additionally, given that the cleaner was likely to spend most of his time in the cleaner room, the mask filtration was not included in estimating the quanta generation. In case that the index case spent half of his time in the seating area and the mask had an infiltration efficiency of 50%, then the estimated quanta generation rate would be 25% higher at 2460 quanta/h.

4.2. Infection prevention is not achieved by ventilation alone

Our study underscores the importance of exchange airflow between zones and the filtration effect of FCUs in the context of infection prevention. When FCUs operated at 41% of the designed flow rate with a PM2.5 filtration efficiency of 21.8%, and when the ventilation systems operated as indicated by the conditions of 1 March 2021, their filtration made contributions to the overall dilution air flow rate of 33.3% in Zone A, 58.9% in Zone B and 56.0% in Zone C. The filtration effect of the fan coil units is considered in our analyses; however, it remains unknown if a FCU can also inactivate virus particles, and further study is needed. In contrast, the contributions of actual outdoor air flow to the overall dilution air flow were only 27.2% in Zone A, 23.4% in Zone B and 36.4% in Zone C. The impact of exchange air flow between zones is complex, as it may involve virus-free airflow, which plays a dilution role, or contaminated airflow, which plays a contamination role. For example, in Zone A, airflow from Zone B to Zone A ($q_{21} = 150$ L/s) acted as a source of infectious quanta emission, while airflow from the shopping arcade to Zone A (237 L/s in $q_{01} = 430$ L/s) played a dilution role similar to that of outdoor airflow, assuming that the shopping arcade air was virus-free. These findings highlight the importance of exchange airflow between zones and FCU filtration in both infection prevention and accurate quanta generation rate estimation during outbreak investigations.

Our study illustrates the difficulty of accurately measuring outdoor air ventilation, exchange airflows between zones and FCU filtration in a multi-zone setting, although the unique feature of co-existing infection and non-infection in three connected restaurant zones was helpful in the outbreak analysis. The restaurant is mechanically ventilated through a central air-conditioning system in a very large shopping centre. The restaurant owner was responsible for ventilation in the restaurant according to local building regulations and thus lacked incentive to collaborate fully in an outbreak investigation. This highlights the urgent need for simple and low-cost methods to replace expensive tracer gas instruments as a means of real-time, automatic monitoring of outdoor airflow and exchange airflow between zones. Furthermore, a device capable of rapidly measuring the equivalent clean air flow rate of any FCU is needed.

4.3. No absolute dilution requirement to avoid secondary infection in a room

The high-end restaurant in this case is located in a large, 10-story, high-class shopping centre that was newly opened in mid-2019. The building service facilities, such as air-conditioning and ventilation, were generally well designed, built and maintained. The occurrence of a large infection outbreak involving 21 patrons was likely to have been due to a super-emitter of infectious virus-containing particles. Our investigation revealed such a possibility, with a quanta generation rate as high as 1968 quanta/h. Even at an approximate exposure duration of 1 h, an equivalent dilution air flow of 20 L/s per person in Zone B was insufficient to avoid virus transmission. A simple estimate can be made using the Wells–Riley equation for a single-zone space with 30 people, each having an inhalation rate of 0.2 L/s and exposure time of 1 h. To avoid secondary infection, the total dilution air flowrate for each person should be as high as 394 L/s. This is in contrast to the typical ventilation requirement of 8–10 L/s per person in an office. For a quanta generation rate of 100 quanta/h and exposure time of 1 h, a dilution air flow rate larger than 10 L/s per person might be sufficient in a large space such as a restaurant to avoid a secondary infection due to long-range airborne exposure. However, for a quanta generation rate of 2000 quanta/h, a dilution air flow rate larger than 200 L/s per person will be needed, which is unrealistically high for typical restaurant settings. ASHRAE 241 [1] requires a “minimum equivalent clean airflow” of 30 L/s per person in restaurants. Avoiding secondary infection in the presence of a super-emitter is probably not possible in a typical air-conditioned building. Fortunately, the purpose of infection control is not limited to achieving zero infection in all buildings, and the number of super-emitters is limited. It might be possible to achieve a reproduction number below 1 in a neighbourhood or a city. To develop city-level ventilation requirements, the quanta generation rate profile of an infected population is needed [48].

4.4. Limitations

This study has several major limitations. First, the precise seating locations of the infected persons at each table and the arrival and departure times of the uninfected patrons are unknown. Real-time data on close contact between the index case and patrons were unavailable due to difficulty accessing CCTV videos. The possibility of failure in wearing mask by the index case cannot be completely ruled out. In our analysis, the short-range airborne route was not considered. Second, the monitored ventilation rates after exposure were used as a proxy for those at the time of exposure, although they might have been modified due to both artificial and operational issues. Thirdly, the exchange flows between Zones B and C were not directly measured during the field experiments due to ignorance. Since the importance of the lack of infection in Zone C was only recognised at the time of analysis. Fourthly, the used tracer gas and fine particles were only proxies for understanding airflow, particle deposition and filtration in our field study, but a bacteria or virus particle tracer would be ideal to be used in future so that the viability loss might be considered. Lastly, a constant inhalation rate of 0.2 L/s for eating activity from US EPA (2021), aerosol deposition rate of 0.3 h⁻¹ and deactivation rate of 0.63 h⁻¹ (Miller et al., 2020) are adopted, and variations in any of these parameters will also lead to changes in the estimated quanta generation rate.

5. Conclusions

A restaurant outbreak of SARS-CoV-2 was investigated through epidemiological, whole-genome sequencing and mechanistic environmental analyses. All analyses revealed that the outbreak was due to a single source, i.e. a cleaner. The outbreak was characterised by the co-existence of infection and non-infection in three connected zones: sec-

ondary infections occurred only in one seating zone. The estimated quanta generation rate of 1968 quanta/h is probably the highest to date among those reported from observed outbreaks of the ancestral strain of SARS-CoV-2. The estimated quanta generation rate was sufficiently high to cause a high attack rate in the affected seating area, but not high enough to cause infection in the other two connected seating areas. The observed high quanta generation rate of the index case suggests that there is probably no required absolute dilution to avoid any secondary infection in an indoor environment. Dilution strategies at building stock scale need to be considered to ensure the reproduction number to be less than one, rather than to avoid secondary infection in all indoor spaces. Both filtration due to FCUs and virus-free exchange air flow from the shopping centre were found to be significant contributors to the overall dilution flow rate in the restaurant. Our finding suggests that multi-zone buildings with central heating, ventilation and air-conditioning systems, the filtration from the devices such as FCUs and dilution due to exchange airflows from neighbouring spaces should be properly accounted for when total effective dilution ability is estimated, particularly in similar outbreak investigations.

Environmental implication

The largest quanta emission rate for SARS-CoV-2 remains unclear, though Cheng et al. [48] estimated a rate of at least 2300 quanta/h for the top 1% of individuals infected with the ancestral strain. However, such a high rate has not been documented in previously reported outbreaks. This study, investigating a SARS-CoV-2 outbreak using epidemiological, whole-genome sequencing and environmental analyses, reports the largest quanta generation rate to date (1968 quanta/h). Our findings suggest that avoiding secondary infection by dilution alone in the presence of a super-emitter might not be possible in typical air-conditioned buildings and other prevention strategies need to be developed.

Uncited references

CRedit authorship contribution statement

Fan Xue: Writing – review & editing, Software, Investigation. **Yuguo Li:** Writing – review & editing, Supervision, Methodology, Funding acquisition, Formal analysis, Conceptualization. **Pak-To Chan:** Software, Investigation. **Peihua Wang:** Software, Methodology, Investigation. **Chung-Hin Dung:** Software, Investigation. **Tiffany Didik:** Resources, Investigation. **Garnet Kwan-Yue Choi:** Resources, Investigation. **Herman Tse:** Resources, Investigation. **Yijie Wu:** Software. **Te Miao:** Writing – review & editing, Investigation. **Wenzhao Chen:** Software, Investigation. **Wei JIA:** Writing – review & editing, Writing – original draft, Visualization, Methodology, Investigation, Formal analysis, Data curation, Conceptualization. **Hua Qian:** Writing – review & editing, Methodology. **Qun Wang:** Writing – review & editing, Methodology, Investigation. **David Christopher Lung:** Writing – review & editing, Resources, Investigation.

Declaration of Competing Interest

The authors declare that they have no known competing financial interests or personal relationships that could have appeared to influence the work reported in this paper.

Acknowledgements

This work was supported by the Research Grants Council of Hong Kong's Collaborative Research Fund (grant number C7104-21G) and a General Research Fund (grant number 17206522).

We thank the relevant staff and management teams of the Food and Environmental Hygiene Department, Environmental Protection Department and Electrical and Mechanical Services Department of Hong Kong Special Administrative Region, China, for their support and data provision during our investigation. We also thank Professor Kwok-Yung Yuen, Dr Kenneth Leung, Professor Patrick Lee and the managers of the shopping centre and the restaurant in facilitating the field study. Professional English language editing support was provided by AsiaEdit (asiaedit.com).

Data Availability

Data will be made available on request.

Appendix A. Supporting information

Supplementary data associated with this article can be found in the online version at doi:10.1016/j.jhazmat.2024.136388.

References

- [1] ASHRAE 241, 2023. ASHRAE Standard 241: Control of Infectious Aerosols. American Society of Heating, Refrigerating and Air-Conditioning Engineers, Georgia, United States.
- [2] Bae S, Kim H, Jung T.Y, Lim J.A, Jo D.H, Kang G.S, et al. Epidemiological characteristics of COVID-19 outbreak at fitness centers in Cheonan, Korea. *J Korean Med Sci* 2020;35(31):e288.
- [3] Bivolarova M, Ondráček J, Melikov A, Ždímal V. A comparison between tracer gas and aerosol particles distribution indoors: the impact of ventilation rate, interaction of airflows, and presence of objects. *Indoor Air* 2017;27(6):1201–12.
- [4] Buonanno G, Stabile L, Morawska L. Estimation of airborne viral emission: quanta emission rate of SARS-CoV-2 for infection risk assessment. *Environ Int* 2020;141:105794.
- [6] Cao Q, Chen A, Zhou J, Chang V.W.C. Performance evaluation of filter applications in fan-coil units during the 2015 Southeast Asian haze episode. *Build Environ* 2016;107:191–7.
- [7] Cap. 132, 2023. Public Health and Municipal Services Ordinance. Available at <https://www.elegislation.gov.hk/hk/cap132>. Accessed 29 May 2024.
- [8] Charlotte N. High rate of SARS-CoV-2 transmission due to choir practice in France at the beginning of the COVID-19 pandemic. *J Voice* 2023;37(2):292–e9.
- [9] Chen Y.C, Yuanhui Z, Barber E.M. A dynamic method to estimate indoor dust sink and source. *Build Environ* 2000;35(3):215–21.
- [10] Cheng V.C.C, Lung D.C, Wong S.C, Au A.K.W, Wang Q, Chen H, et al. Outbreak investigation of airborne transmission of Omicron (B. 1.1. 529)-SARS-CoV-2 variant of concern in a restaurant: Implication for enhancement of indoor air dilution. *J Hazard Mater* 2022;430:128504.
- [11] Diapouli E, Chaloulakou A, Koutrakis P. Estimating the concentration of indoor particles of outdoor origin: a review. *J Air Waste Manag Assoc* 2013;63(10):1113–29.
- [12] Du Z, Xu X, Wu Y, Wang L, Cowling B.J, Meyers L.A. Serial interval of COVID-19 among publicly reported confirmed cases. *Emerg Infect Dis* 2020;26(6):1341–3.
- [13] Fears A.C, Klimstra W.B, Duprex P, Hartman A, Weaver S.C, Plante K.S, et al. Persistence of severe acute respiratory syndrome coronavirus 2 in aerosol suspensions. *Emerg Infect Dis* 2020;26(9):2168–71.
- [14] Gavin, H.P., 2019. The Levenberg-Marquardt algorithm for nonlinear least squares curve-fitting problems. *Department of Civil and Environmental Engineering, Duke University*. [Online]. Available: <https://people.duke.edu/~hpgavin/lm.pdf>. Accessed 29 June 2021.
- [15] He X, Lau E.H, Wu P, Deng X, Wang J, Hao X, et al. Temporal dynamics in viral shedding and transmissibility of COVID-19. *Nat Med* 2020;26(5):672–5.
- [16] <https://www.info.gov.hk/gia/general/202007/27/P2020072700650.htm>.
- [17] <https://www.info.gov.hk/gia/general/202102/17/P2021021700662.htm>.
- [18] https://www.fehd.gov.hk/english/licensing/guide_general_reference/report_air-changes_purification.html.
- [19] <https://www.info.gov.hk/gia/general/202302/28/P2023022800677.htm>.
- [20] Huang W, Wang K, Hung C.T, Chow K.M, Tsang D, Lai R.W.M, et al. Evaluation of SARS-CoV-2 transmission in COVID-19 isolation wards: on-site sampling and numerical analysis. *J Hazard Mater* 2022;436:129152.
- [21] Jia W, Cheng P, Ma L, Wang S, Qian H, Li Y. Individual heterogeneity and airborne infection: effect of non-uniform air distribution. *Build Environ* 2022;226:109674.
- [22] Kang C.R, Lee J.Y, Park Y, et al. Coronavirus disease exposure and spread from nightclubs, South Korea. *Emerg Infect Dis* 2020;26(10):2499–501.
- [23] Kim J.H, Kwok K.O, Huang Z, Poon P.K.M, Hung K.K.C, Wong S.Y.S, et al. A longitudinal study of COVID-19 preventive behavior fatigue in Hong Kong: a city with previous pandemic experience. *BMC Public Health* 2023;23(1):618.
- [24] Koutrakis P, Briggs S.L, Leaderer B.P. Source apportionment of indoor aerosols in Suffolk and Onondaga Counties, New York. *Environ Sci Technol* 1992;26(3):521–7.
- [25] Li Y, Huang X, Yu I.T, Wong T.W, Qian H. Role of air distribution in SARS

- transmission during the largest nosocomial outbreak in Hong Kong. *Indoor Air* 2005;15(2).
- [26] Li Y, Leung M, Tang J.W, Yang X, Chao C.Y.H, Lin J.Z, et al. Role of ventilation in airborne transmission of infectious agents in the built environment – a multidisciplinary systematic review. *Indoor Air* 2007;17(1):2–18.
- [27] Li Y, Qian H, Hang J, Chen X, Cheng P, Ling H, et al. Probable airborne transmission of SARS-CoV-2 in a poorly ventilated restaurant. *Build Environ* 2021; 196:107788.
- [28] Miller S.L, Leiserson K, Nazaroff W.W. Nonlinear least-squares minimization applied to tracer gas decay for determining air flow rates in a two-zone building. *Indoor Air* 1997;7(1):64–75.
- [29] Miller S.L, Nazaroff W.W, Jimenez J.L, Boerstra A, Buonanno G, Dancer S.J, et al. Transmission of SARS-CoV-2 by inhalation of respiratory aerosol in the Skagit Valley Chorale superspreading event. *Indoor Air* 2021;31(2):314–23.
- [30] Morawska L, Allen J, Bahnfleth W, Bluyssen P.M, Boerstra A, Buonanno G, et al. A paradigm shift to combat indoor respiratory infection. *Science* 2021;372(6543): 689–91.
- [31] Ou C, Hu S, Luo K, Yang H, Hang J, Cheng P, et al. Insufficient ventilation led to a probable long-range airborne transmission of SARS-CoV-2 on two buses. *Build Environ* 2022;207:108414.
- [32] Qian H, Li Y, Nielsen P.V, Huang X. Spatial distribution of infection risk of SARS transmission in a hospital ward. *Build Environ* 2009;44(8):1651–8.
- [33] Qian H, Zheng X. Ventilation control for airborne transmission of human exhaled bio-aerosols in buildings. *J Thorac Dis* 2018;10(19):S2295.
- [34] Riley E.C, Murphy G, Riley R.L. Airborne spread of measles in a suburban elementary school. *Am J Epidemiol* 1978;107(5):421–32.
- [35] Sherman M.H. Tracer-gas techniques for measuring ventilation in a single zone. *Build Environ* 1990;25(4):365–74.
- [36] Si X, Xi J.S, Talaat M, Park J.H, Nagarajan R, Rein M, et al. Visualization and quantification of facemask leakage flows and interpersonal transmission with varying face coverings. *Fluids* 2024;9(7):166.
- [37] Solano T, Ni C, Mittal R, Shoel K. Perimeter leakage of face masks and its effect on the mask's efficacy. *Phys Fluids* 2022;34(5).
- [38] Sun Y, Wang Z, Zhang Y, Sundell J. In China, students in crowded dormitories with a low ventilation rate have more common colds: evidence for airborne transmission. *PloS One* 2011;6(11):e27140.
- [39] Thatcher T.L, Lai A.C, Moreno-Jackson R, Sextro R.G, Nazaroff W.W. Effects of room furnishings and air speed on particle deposition rates indoors. *Atmos Environ* 2002;36(11):1811–9.
- [40] U.S. EPA., 2011. Exposure factors handbook: 2011 edition. National Center for Environmental Assessment, Washington, DC; EPA/600/R-09/052 F. Available from the National Technical Information Service, Springfield, VA, and online at <http://www.epa.gov/ncea/efh>.
- [41] Van Doremalen N, Bushmaker T, Morris D.H, Holbrook M.G, Gamble A, Williamson B.N, et al. Aerosol and surface stability of SARS-CoV-2 as compared with SARS-CoV-1. *N Engl J Med* 2020;382(16):1564–7.
- [42] Vernez D, Schwarz S, Sauvain J.J, Petignat C, Suarez G. Probable aerosol transmission of SARS-CoV-2 in a poorly ventilated courtroom. *Indoor Air* 2021;31(6):1776–85.
- [43] Wang C.C, Prather K.A, Sznitman J, Jimenez J.L, Lakdawala S.S, Tufekci Z, et al. Airborne transmission of respiratory viruses. *Science* 2021;373(6558):eabd9149.
- [44] Wells W.F. Airborne Contagion and Air Hygiene: An Ecological Study of Droplet Infections. Cambridge, MA: Harvard University Press; 1955.
- [45] Zhang C, Nielsen P.V, Liu L, Sigmer E.T, Mikkelsen S.G, Jensen R.L. The source control effect of personal protection equipment and physical barrier on short-range airborne transmission. *Build Environ* 2022;211:108751.
- [46] Zhang N, Chen X, Jia W, Jin T, Xiao S, Chen W, et al. Evidence for lack of transmission by close contact and surface touch in a restaurant outbreak of COVID-19. *J Infect* 2021;83(2):207–16.
- [48] Cheng P, Jia W, Liu L, Yen H.L, Li Y. A power-law distribution of infectious quanta for the top 30% of SARS-CoV-2-infected individuals. *Building and Environment* 2024;112256.